J Mol Model (2011) 17:2275–2284
DOI 10.1007/s00894-010-0864-8

ORIGINAL PAPER

Computational prediction of selectivities in nonreversible and reversible hydroformylation reactions catalyzed by unmodified rhodium-carbonyls

Giuliano Alagona · Raffaello Lazzaroni · Caterina Ghio

Received: 15 September 2010 / Accepted: 28 September 2010 / Published online: 3 November 2010

Abstract The regio- and stereoselectivities of the hydroformylation reaction catalyzed by an unmodified Rh catalyst have been investigated at the B3P86/6-31G* level with Rh described by effective core potentials in the LANL2DZ valence basis set for a number of either mono- or (1,1-, 1,2-, 1,3-) di-substituted substrates and compared with a variety of earlier results of ours, supplemented with free energy results when not already available. The computational prediction of regio- and stereoselectivities in nonreversible hydroformylations performed under mild reaction conditions is seemingly possible provided a careful conformational search for TS structures is carried out and all the low energy conformers are taken into account. The internal energy can be used to compute both the regio- and stereoselectivities in the hydroformylation of 1,1- and 1,3-substituted substrates with satisfactory results, whereas for 1,2-substituted substrates the regioselectivity determined from the internal energy is in good agreement with the experiment in the case of aliphatic olefins just for the lowest terms in the series (i.e., methyl and ethyl substituents), while the ratios are only qualitatively correct for the slightly bulkier iso-propyl and tert-butyl moieties. The theory/experiment agreement becomes decidedly better using the free energy differences instead.

Keywords B3P86/6-31G*/LanL2DZ · Hydroformylation · Regioselectivity · 3,4-dimethyl-pent-1-ene · 3-methyl-but-1-ene · 3-methyl-pent-1-ene · 3-phenyl-but-1-ene · 3-phenyl,4-methyl-pent-1-ene 3-phenyl-pent-1-ene · 3-phenyl,4,4-dimethyl-pent-1-ene · 3,4,4-trimethyl-pent-1-ene

G. Alagona (✉) · C. Ghio (✉)
Molecular Modeling Lab,
CNR-IPCF (Institute for Physico-Chemical Processes),
Via Moruzzi 1,
56124 Pisa, Italy
e-mail: G.Alagona@ipcf.cnr.it
e-mail: C.Ghio@ipcf.cnr.it

R. Lazzaroni
DCCI (Department of Chemistry and Industrial Chemistry),
University of Pisa,
Via Risorgimento 35,
56126 Pisa, Italy

Introduction

The hydroformylation reaction is a typical homogeneous process used to produce aldehydes, catalyzed by transition metal complexes, primarily low valent cobalt or rhodium catalysts. In the latter case, especially Rh(I) complexes (unmodified or modified with phosphine ligands) are employed. In general, phosphine-modified rhodium catalysts are preferred because the steric hindrance of bulky groups might help selectivity; they are active however under severe reaction conditions only (T≥100 °C), whereas with unmodified Rh catalysts the reaction occurs in a wide majority of cases at room temperature (rt) or at T ≤60 °C at most. The unmodified catalytic precursor [$Rh_4(CO)_{12}$] produces, under mild hydroformylation conditions, a Rh-carbonyl hydride [$H{-}Rh(CO)_3$], which is the catalytic active species in the reaction. From the computational viewpoint, the absence of phosphines reduces the system complexity and the number of isomers to be considered. Moreover, since the reaction occurs at rt, a consistent comparison between theoretical and experimental results can be performed. Because of the economic value of the aldehydes (and mainly of the corresponding alcohols, widely employed for several applications and in the fragrance industry) produced, it is of

paramount importance the control of reaction selectivities, i.e., regioselectivity (B:L, Scheme 1) as well as diastereoselectivity (b:b′, Scheme 2, showing two peculiar systems) when the substrate is a chiral compound.[1]

Since the earlier theoretical studies on hydroformylation [1–6], discussed in an excellent review [7], an increasing number of articles have been devoted to elucidate the metal-catalyzed hydroformylation mechanism with computational methods [8–27] employing either phosphine-modified (sometimes also heterobimetallic) or unmodified catalysts. The mechanism was investigated with a variety of computational approaches and substrates as well, including ethene [3–6, 10–13, 17, 21, 25], the smaller substrate that however cannot show any selectivity. Employing the next olefin, propene [5, 8, 10, 12, 27], regioselectivity can be considered, as can be easily derived from Scheme 1.

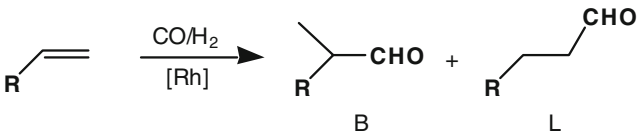

Scheme 1 Hydroformylation of a terminal olefin. Branched and linear aldehydes are produced for R≠H.

We addressed the regioselectivity issue for a series of eight mono-substituted olefins plus ethene and dimethylethene in the presence of an unmodified rhodium catalyst in our first study on hydroformylation [12], where in order to validate the computational strategy the B:L regioisomeric ratio was theoretically evaluated from both the internal and free energy differences of branched and linear alkyl-rhodium transition states (TS):

$$\mathrm{B:L} = k_{\mathbf{B}} : k_{\mathbf{L}} = \sum \mathrm{k}_B[\mathrm{C}] : \sum \mathrm{k}_L[\mathrm{C}] = \sum e^{-\Delta \mathrm{G}_{\mathrm{B}}^{\neq}/\mathrm{RT}} : \sum e^{-\Delta \mathrm{G}_{\mathrm{L}}^{\neq}/\mathrm{RT}} = \sum e^{-\Delta\Delta \mathrm{G}^{\neq}/\mathrm{RT}} \approx \sum e^{-\Delta\Delta \mathrm{E}^{\neq}/\mathrm{RT}} \quad (1)$$

(where k = reaction rate, k = rate constant, [C] = concentration of the olefin-Rh complex, $\Delta G^{\neq}$ = TS free energy, $\Delta E^{\neq}$ = TS internal energy). Zero-point energies and thermal corrections were computed in the rigid rotor-harmonic oscillator approximation to obtain free energies [28]. By comparing theoretical and experimental results, we demonstrated that the nonreversible olefin insertion into the Rh–H bond was the step determining the regioselectivity. Furthermore, both the internal and free energy gaps were very close to the experimental result for all the substrates considered, but for 1-hexene whose free energy-based regioisomeric ratio (10:90) turned out to be far from the experimental value (48:52), whereas the internal energy-based ratio was 50:50. The likely reason of this failure for the most flexible substrate was attributed to hindered rotations taken as real vibrations.

Therefore, in our subsequent studies of nonreversible hydroformylations for the substrates displayed in Scheme 2 [15, 19], which represent interesting cases of substrate asymmetric inductions, the internal energy-based values were adopted, because also the theoretical diastereomeric ratios can be evaluated with an expression analogous to that reported in Eq. 1:

$$\mathrm{b:b'} = k_{\mathrm{b}} : k_{\mathrm{b'}} = \sum e^{-\Delta \mathrm{G}_{\mathrm{b}}^{\neq}/\mathrm{RT}} : \sum e^{-\Delta \mathrm{G}_{\mathrm{b'}}^{\neq}/\mathrm{RT}} = \sum e^{-\Delta\Delta G^{\neq}/\mathrm{RT}} \approx \sum e^{-\Delta\Delta E^{\neq}/\mathrm{RT}} \quad (2)$$

and the theoretical values turned out to be in good agreement with the relevant experimental results [15]. In addition, even considering as a substrate a 1,2-disubstituted compound, i.e., with the stereocenter directly linked to the olefin double bond without any X separator, only limited changes in the computed ratios were obtained [19], although without the possibility to compare the result to experiment, because the experimental value for that substrate was not available at that moment. Both ratios indicated however scarce selectivity as expected.

Among disubstituted substrates, a few 1,3-, 1,2-, and also 1,1-disubstituted compounds have been examined thus far, although it is well known that aryl and alkyl 1,1-disubstituted olefins produce the linear aldehydes as the only product. In the case of 1,1-dimethylethene, regioisomeric ratios of 9:91 and 10:90 derive from the TS internal and free energy gaps, respectively, in satisfactory agreement with the 1:99 experimental ratio [12]. Conversely, for other 1,1-disubstituted substrates, for which the reaction is probably reversible, theoretical B:L ratios turn out to be 50:50 or even 72:28 as in the case of 1,1-diphenylethene,

[1] Actually a chiral center appears in the hydroformylation of a nonchiral substrate when R (Scheme 1) is an alkyl group greater than CH_3 or an aromatic group; the hydroformylation with unmodified rhodium catalysts however produces the racemic branched aldehydes without any stereoselectivity. In contrast, when the substrate is a chiral olefin itself, diastereoselectivity might originate as shown for two 1,3-substituted olefins in Scheme 2; notice that in such cases the total branched population is used to obtain the regioselectivity, because $\mathrm{b} + \mathrm{b'} = \mathrm{B}$.

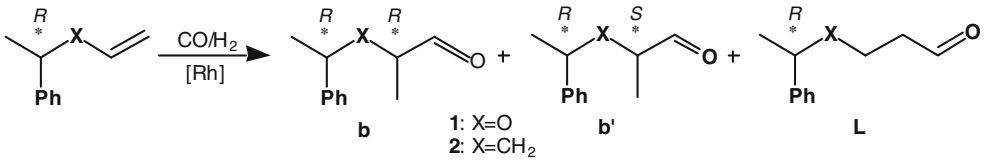

Scheme 2 Hydroformylation of two particular chiral (*R*) substrates, according to the nature of X. Two branched diastereomers, *RR* (b) and *RS* (b′) and the linear aldehyde can be obtained for each of them.

instead. This fact prompted us to take into account the whole reaction mechanism [23], providing a synthetically unprecedented explanation of this behavior: the free energy profiles put forward that β-hydride elimination, which is clearly due to the TS for the CO addition, occurs only along the branched pathway. When studying the whole reaction mechanism it is of course necessary to consider the free energy of the system, because the number of species changes along the path. As a byproduct of that investigation, however, we noticed that remarkable differences were obtained between TS internal energies and free energies.

Therefore the limits of validity of the internal energy approximation even on the first step TS were to be further investigated. To this end, we consider two sets (R=CH_3 and R=C_6H_5) of 1,2-disubstituted compounds (R′=CH_3, C_2H_5, $CH(CH_3)_2$ or $C(CH_3)_3$) (Scheme 3) and discuss the results obtained with an eye to our earlier results.

Computational details

All the calculations have been performed with the Gaussian 03 codes [29], in the density functional theory (DFT) framework, making use of B3P86, i.e., the Becke gradient-corrected three-parameter hybrid exchange and Perdew 86 gradient-corrected correlation functionals [30, 31]. Coupled to the B3P86/6-31G* [32] description for C, O and H, effective core potentials that implicitly include some relativistic effects for the electrons near the nucleus in the LanL2DZ valence basis set have been used for Rh [33]. The results of a few calculations making use of different pseudopotentials on all atoms but H (*vide infra*) and B3LYP [30, 34] are also briefly discussed for comparison.

Results and discussion

Hydroformylation regioselectivity for one-substituted and 1,1-disubstituted olefins

For all the substrates considered in Ref. 12, the agreement between theory and experiment is good both considering energy and free energy, as can be derived from a perusal of Table 1, with a single exception, namely when the substrate is 1-hexene, presumably because in the vibrational analysis of the Rh-tricarbonyl TS complexes of such a flexible substrate hindered rotations of the long aliphatic chain were taken as real vibrations. Actually, in that case, the experimental value is well reproduced by the internal energy difference between all the branched and linear TS structures. The calculation of vibrational frequencies furthermore confirmed the TS nature of the stationary points found. Interestingly, as stated in the introduction, the computed 1,1-dimethylethene regioselectivity ratio turned out to be in satisfactory agreement with the experimental value.

In contrast, in the case of 1,1-diphenylethene the internal energy-based theoretical prediction (72:28) was opposite to the experimental value at complete substrate conversion. The free energy-based theoretical prediction of the regioselectivity ratios was slightly better, but still 61:39 and 56:44 at 298 and 373 K, respectively.

The origin of this behavior was to be sought in the subsequent reaction steps, still the branched and linear profiles relaying only on intermediates and TS were unable to explain the reaction outcome. The stability of the tetracarbonyl complexes, easily obtained from model-built starting structures, suggested the presence of vanishingly small barriers between them and the tricarbonyl ones. By examining the Rh-tricarbonyl complexes (Fig. 1), however, a remarkable difference between the branched and linear structures was evident, that indicated a likely barrier along the branched path for the incoming CO, due to the agostic interaction of Rh with one of the phenyl ring π density. The CO approaching paths showed indeed a much higher barrier for the branched than for the linear complexes. The addition of the relevant TS to the linear and branched profiles, especially considering the free energy, necessary because of the change in the number of species along the pathway, allowed us to explain at which stage β-hydride elimination takes place [23, 26].

The upward shift of about 10 kcal mol^{-1} obtained in the branched free energy profile upon addition of the fourth CO group was maintained for all the forthcoming steps (Fig. 2). Actually the superimposition of the branched and linear free energy profiles at 373 K making the tetra-carbonyl complexes coincide did not show remarkable differences between the two pathways [see Fig. 7 of Ref. 23].

Scheme 3 Hydroformylation of 1,2-disubstituted substrates

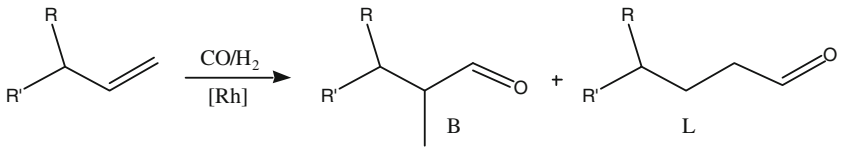

Therefore already the TS for the CO insertion along the branched free energy-based pathway turned out to be significantly higher than the alkyl-Rh TS, suggesting that most of the branched conformers leave their pathway and return to reactants with an enrichment in the linear products. It is thus irrelevant that the next TS (H_2 addition and H reductive elimination) are even higher than the CO insertion one [23, 26].

Hydroformylation regio- and diastereoselectivity for 1,3-disubstituted olefins

In the case of the substrates displayed in Scheme 2, the internal energy-based selectivity ratios have been computed with two different combinations of functionals and effective core potentials (ECP), namely B3LYP/SBK(d)[2] (making use of ECP for Rh and main group atoms) and B3P86/6-31 G* (with ECP on Rh coupled to the LanL2DZ valence basis set) [19]. The results reported in the two upper rows of Table 2 indicate that the values are not particularly sensitive to the theoretical description employed, that however are both decidedly reliable [11, 19].

The agreement between theoretical and experimental regio- and diastereoselectivities is fairly satisfactory even considering the internal energy gaps at the TS level for 1,3-disubstituted substrates. Roughly speaking, the large separation between substituent and catalytic groups might explain the reaction outcome. The major difference is due to the nature of the X separator: the CH_2 group acts as an insulator, producing scarce selectivities, while the ethereal O favors cis/trans arrangements remarkably increasing regio- and diastereoselectivities. Even the substrate without any X separator (a 1,2-disubstituted substrate is also reported in Table 2) is predicted to yield a very low selectivity (no stable experimental values are available for that substrate).

Hydroformylation regioselectivity for 1,2-disubstituted olefins

Two sets of 1,2-disubstituted olefins (for their definition refer to Scheme 3) have thus been taken into account from both the experimental and computational viewpoints. In the first set, the R substituent is the methyl group (Me), while in the second one it is the phenyl ring (Φ) producing either a fully aliphatic or a partially aromatic class of compounds. Four different R′ moieties have been then substituted to the common skeletons; they are in turn the methyl (Me), ethyl (Et), *iso*-propyl (iPr), and *tert*-butyl (tBu) groups.

Although in this series the substrate is achiral only when R = R′ = Me (i.e., in 3-methyl-but-1-ene), we limit ourselves to discuss the regioselectivity ratio. In what follows, the substrates are referred to either with their names or as R = Me/Φ, R′ = Me/Et/iPr/tBu (i.e., 3-methyl-pent-1-ene is R = Me, R′ = Et; 3,4-dimethyl-pent-1-ene is R = Me, R′ = iPr; 3,4,4-trimethyl-pent-1-ene is R = Me, R′ = tBu; (1-methyl-allyl)-benzene is R = Φ, R′ = Me (or 3-phenyl-but-1-ene); (1-ethyl-allyl)-benzene is R = Φ, R′ = Et (or 3-phenyl-pent-1-ene); (1-*i*propyl-allyl)-benzene is R = Φ, R′ = iPr (or 3-phenyl,4-methyl-pent-1-ene); (1-*t*butyl-allyl)-benzene is R = Φ, R′ = tBu (or 3-phenyl,4,4-dimethyl-pent-1-ene)).

Apart from the intrinsic group size, the computational effort increases with the number of possibly different conformers, which is limited for Me and tBu because of the group symmetry and thrice as much[3] for Et and iPr as shown in Fig. 3 for the (1-ethyl-allyl)-benzene substrate. The same holds for (1-isopropyl-allyl)-benzene, as it is evident by replacing Et with iPr in the three top projections of this figure, and methyl groups to the hydrogens and vice versa on the C toward the observer in the nine bottom projections.

All the possible conformers must be taken into account not to miss any important contributor to the branched or linear population. It is noteworthy that such a variety of structures must be taken into account for each type of complex (i.e., b, b′, l, l′). Of course, not all of the investigated structures are found to be local TS due to the possible steric hindrance, although invariably all model-built TS geometries have been optimized first as minima by imposing proper constraints that then have been relieved when optimizing as TS.

[2] The SBK(d) basis set is described in detail in Ref. 11.

[3] In those cases, 36 complex structures can be obtained, nine for each type (b, b', l, l'). Taking into account the possible switch of the apical CO, as we did, the total number becomes 72.

Table 1 B3P86/6-31G* regioisomeric ratios based on relative energies or free energies (Eq. 1) for the TS complexes of the substrates indicated. The experimental values are reported for comparison

B3P86/6-31G*	B:L (ΔE)	B:L (ΔG)	B:L (exp)
propene	56:44	59:41	50:50
1-hexene	50:50	10:90	48:52
3,3-dimethylbutene	15:85	9:91	10:90
F-ethene	98:2	97:3	100:0
3,3,3-trifluoropropene	98:2	97:3	97:3
vinylmethylether	86:14	95:5	83:17
allylmethylether	87:13	88:12	70:30
styrene	98:2	98:2	98:2
1,1-dimethylethene	9:91	10:90	1:99

Substrates with R = Me

The schematic structures of the TS complexes for this set of substrates can be obtained by replacing the phenyl ring with a methyl group in Fig. 3. The internal energy-based regioselectivity ratios for this set of substrates, reported in Table 3, are fairly satisfactory when R′ = Me or Et, whereas for iPr and tBu the linear products prevail only slightly over the branched ones and thus agreement with the experimental values can be fortuitous.

Deuterioformylation experiments pointed out reaction reversibility, i.e., β-hydride elimination, or β-elimination for short, primarily when tBu is present [35]. Conversely, for the substrate containing iPr, the experimental results were affected by a remarkable uncertainty, showing variable outcomes. Therefore little β-elimination should occur in the hydroformylation of the iPr-substituted substrate, if any. On the other hand, the almost perfect agreement between free energy-based and experimental values for this substrate supports the lack of β-elimination. Interestingly, apart the first term in the series, there is a significant improvement if the free energy-based regioselectivity ratios are used, indicating that the entropy effect is large for bulky groups.

In an attempt of evaluating entropic contributions, we resorted to the Arrhenius equation

$$k = Ae^{-E_a^{\neq}/RT} \tag{3}$$

pre-exponential frequency factor A, that can be expressed as [36]

$$A = \frac{\prod_{i=1}^{s} \nu_i^{\mathrm{Reac}}}{2\pi \prod_{i=1}^{s-1} \nu_i^{\neq}} \tag{4}$$

and the productories run over all the real frequencies for the reactants and the TS. Since we are interested in the B:L ratio, assuming

$$K = A_B/A_L \tag{5}$$

then the reactant frequencies need not to be computed, because

$$K = \prod_{i=1}^{s-1} \left[\nu_i^{\neq}\right]_L / \prod_{i=1}^{s-1} \left[\nu_i^{\neq}\right]_B \tag{6}$$

considering only the most favorable TS of each type. Hence, $K>1$ when $A_B>A_L$ or

$$\prod_{i=1}^{s-1} \left[\nu_i^{\neq}\right]_L > \prod_{i=1}^{s-1} \left[\nu_i^{\neq}\right]_B \tag{7}$$

and $K<1$ when $A_B<A_L$ or

$$\prod_{i=1}^{s-1} \left[\nu_i^{\neq}\right]_L < \prod_{i=1}^{s-1} \left[\nu_i^{\neq}\right]_B. \tag{8}$$

By applying the outlined procedure to the aliphatic substrates, the values reported in Table 4 have been obtained. For the sake of consistency, the last four columns contain values computed employing only the two most favorable TS of each type.

The productories have been calculated using the wave numbers (cm^{-1}, instead of sec^{-1}, because the ratio is independent of the unit).[4] The regioselectivity ratios based on the internal energy or the free energy are noticeably different especially for the higher terms in the set (iPr and tBu). It is worth noticing that the free energy-based values are even less sensitive to the number of conformers considered than the internal energy-based ones: this result might however be fortuitous and should be further checked. Anyway, by multiplying the internal energy-based K by the relevant K factors calculated from the productory ratio, values close to the free energy-based K are obtained. This fact confirms if necessary that the approach followed is meaningful.

Conversely, more difficult it was to find a correlation with the IR vibrational spectra. From a perusal of the frequencies, the main changes have been found in general in the region 300-1100 cm^{-1}. Therefore, those sections of the IR spectra are displayed in Fig. 4 for the lowest TS along the branched and linear pathways (i.e., TSB and TSL) for the set of compounds under scrutiny.

[4] For the productories, both the B and L values are reported without an identical 10^n factor.

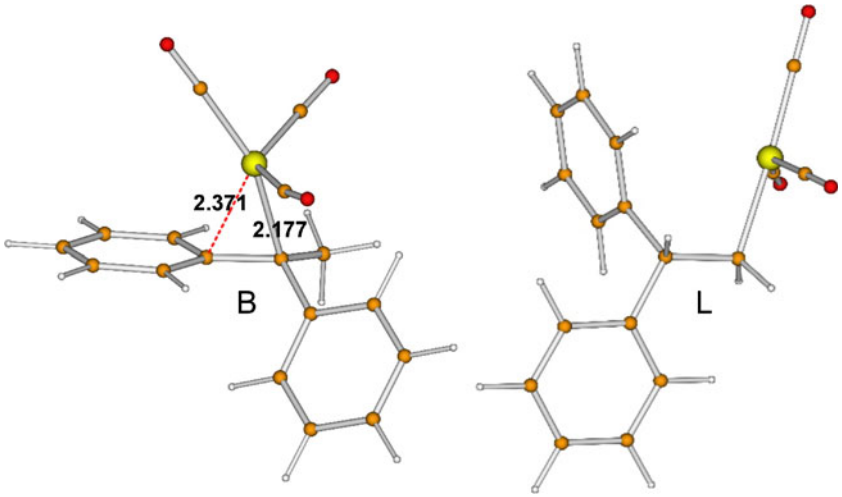

Fig. 1 B3P86/6-31G*/LanL2DZ most favorable branched and linear Rh-tricarbonyl complex structures of the 1,1-diphenylethene substrate

By comparing the spectra, the main changes are found in the TSL for the iPr-substituted compound. The peak at 781 cm^{-1} in the tBu-substituted compound corresponding to the wagging of the H bonded to the Rh atom appears as a very small hump at 746 cm^{-1} in the iPr-substituted compound.

Substrates with R = Φ

For this set of substrates, the preliminary experimental results are confirmed only for the tBu-substituted compound, where β-elimination has also been found [37]. Therefore they are not reported in Table 5 together with the computed results. They put forward a limited selectivity, at least for the first three substrates in this set, with the linear path additionally favored over the branched one with respect to the R = Me substrate. In our opinion, the computed results are reliable, even though they do not significantly differ from those obtained for the aliphatic substrates discussed in the previous section. Also for this set of substrates, β-elimination seemingly occurs only for the tBu-substituted compound.

To show the effect of not including all the TS in the regioselectivity calculation on the final value, as an example, only the four most stable TS complexes for the (1-ethyl-allyl)-benzene substrate are reported in Fig. 5 for the sake of comparison with the relevant data in Table 5. In this case the ratio exploiting only the most stable TS of each type comes out 52:48, still close to 50:50, although reversed with respect to the 47:53 value obtained making use of all the conformers for each type of linear and branched arrangements. In other cases the difference is much more evident, as we found in Ref. 12 and in vinyl ethers [15]. Other authors as well stress the importance of using all the TS structures in the calculation of the selectivity [14]. Anyway, since all the possible TS con-

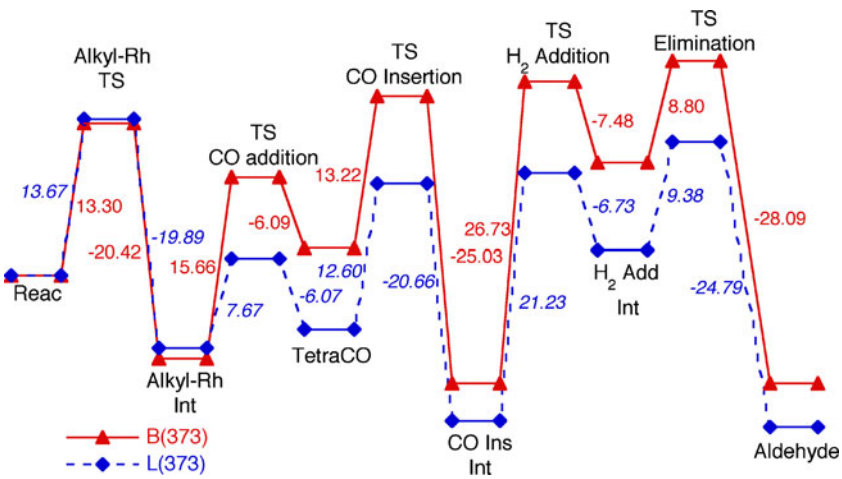

Fig. 2 B3P86/6-31G*/LanL2DZ free energy profiles for the complete hydroformylation reaction mechanism of the 1,1-diphenylethene substrate

Table 2 B3LYP/SBK(d) and B3P86/6-31G* selectivity ratios based on relative energies or free energies (Eqs. 1 and 2) for the TS complexes of the substrates indicated

	B:L (ΔE)		B:L (exp)	b:b′ (ΔE)		b:b′ (exp)
	B3LYP/SBK(d)	B3P86/6-31G*		B3LYP/SBK(d)	B3P86/6-31G*	
(1-vinyloxy-ethyl)-benzene	72:28	89:11	85:15	97:3	96:4	88:12
(1-methyl-but-3-enyl)-benzene	50:50	48:52	49:51	55:45	56:44	52:48
(1-methyl-allyl)-benzene	44:56	44:56		39:61	44:56	

formers must be computed in order to locate the most stable ones, it is obvious that an insignificant saving of time is obtained in disregarding most of them in the calculation of the population.

After the successful estimate of the reaction free energy made by Morokuma and co-workers [4], van Leeuwen et al. [38] suggested to use free energy profiles to discuss kinetics and reaction mechanisms. Free energy values thus assumed an increasing importance and, besides us [12, 23, 26], a number of other authors [14, 18, 21, 25] reported them. Conversely, a few studies performed the vibrational frequency analysis to characterize the nature of the stationary points located on the potential energy surface or to add zero point energy corrections [8, 11, 13, 16, 27]. It is worth noting that when the free energy computed via vibrational frequency analysis in the rigid rotor-harmonic oscillator approximation is not adequate to reproduce correct experimental values, the reason might reside in the hindered rotations considered as real vibrations [12]. In other cases, the use of the internal energy can provide a satisfactory approximation to the free energy-based selectivity ratios [12]. The thorough examination of the behavior of two classes of 1,2-disubstituted substrates performed herein permits us to state that, at least for the alkyl system (R=Me) for which the experimental values are available, the free energy-based regioselectivity ratios are much better in line with the experiment than the internal energy-based ones, and are correct unless β-elimination occurs. This was observed earlier in the case of 1,1-diphenylethene [23, 26]. New results will be reported soon for interesting cyclic substrates [39].

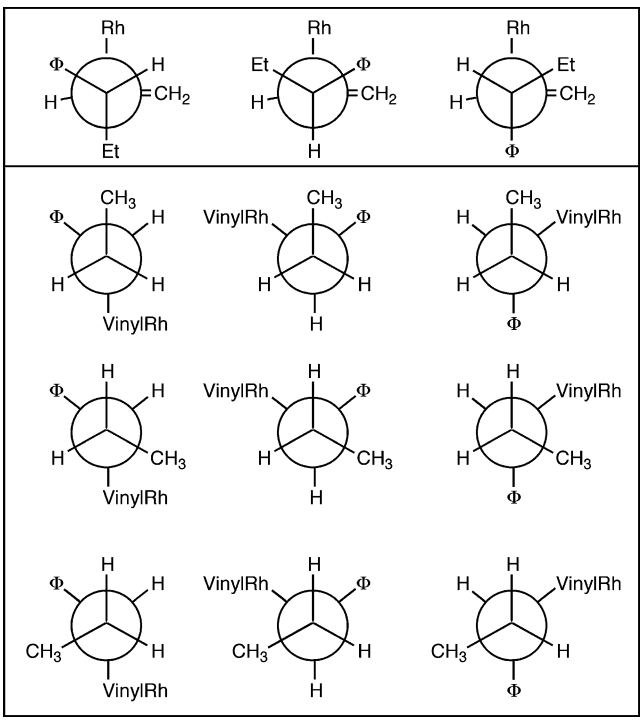

Fig. 3 Newman projections for the TSB (and TSL) complexes of Rh $(CO)_3$-with the (1-ethyl-allyl)-benzene substrate. The same holds for (1-isopropyl-allyl)-benzene, as it is evident by replacing Et with iPr in the three top projections of this figure, and methyl groups to the hydrogens and vice versa on the C toward the observer in the nine bottom projections

Concluding remarks

The assumption that the internal energy can be a satisfactory approximation to the free energy in the determination of the selectivity ratios via a Boltzmann distribution of the TS populations has been validated for a number of

Table 3 B3P86/6-31G* regioisomeric ratios based on relative energies or free energies (Eq. 1) for the TS complexes of the substrates indicated (Scheme 3). The experimental values are reported for comparison

R=Me	B:L (ΔE)	B:L (ΔG)	B:L (exp)
R′=Me	38:62	38:62	38:62
R′=Et	38:62	34:66	34:66
R′=iPr	42:58	32:68	30:70
R′=tBu	47:53	15:85	5:95

Table 4 B3P86/6-31G* branched and linear Arrhenius pre-exponential factors, productories of the TS frequencies (excluding the imaginary frequency), *K* (Eq. 5) regioisomeric ratios based on relative energies or free energies for the most stable TS complexes of each type

R=Me	$\Pi_L \nu^{\neq}$	$\Pi_B \nu^{\neq}$	*K*	B:L (Δ*E*)	B:L (Δ*G*)	*K* (Δ*E*)	*K* (Δ*G*)
R′=Me	14.7	13.6	1.080	47:53	48:52	0.880	0.938
R′=Et	46.1	64.7	0.712	48:52	34:66	0.927	0.508
R′=iPr	18.9	34.0	0.555	48:52	32:68	0.919	0.477
R′=tBu	43.6	259.3	0.168	55:45	14:86	1.227	0.160

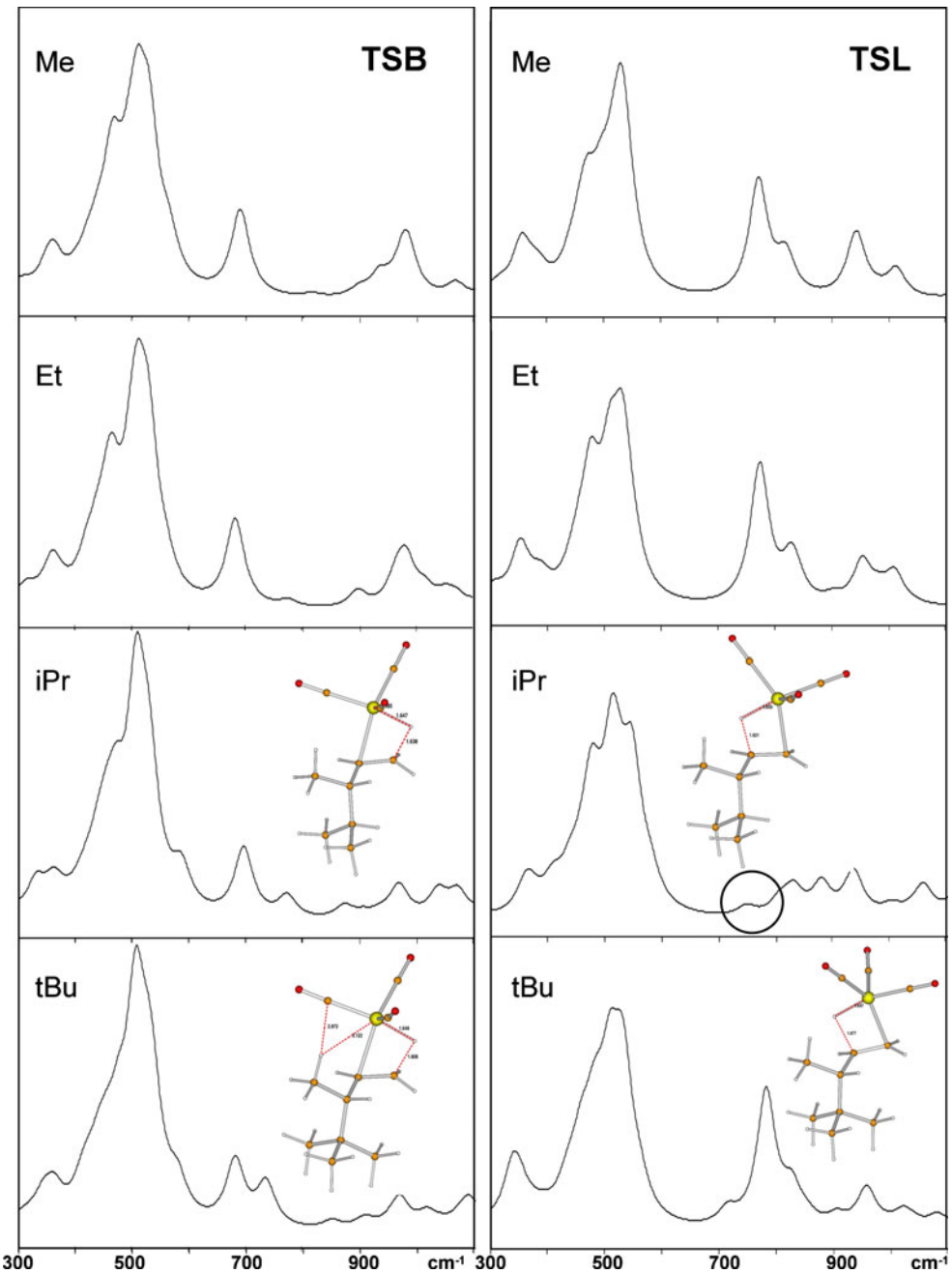

Fig. 4 B3P86/6-31G*/LanL2DZ IR spectra in the region 300-1100 cm^{-1} for the lowest energy TS complexes of the alkyl substrates considered

Table 5 B3P86/6-31G* regioselectivity ratios based on relative energies or free energies (Eqs. 1 and 2) for the TS complexes of the aryl substrates indicated

R=Φ	B:L (Δ*E*)	B:L (Δ*G*)	B:L (exp)
R′=Me	44:56	34:66	–
R′=Et	47:53	24:76	–
R′=iPr	45:55	26:74	–
R′=tBu	50:50	20:80	5:95

disubstituted compounds. The computational prediction of regio- and stereoselectivities in the nonreversible hydroformylation of 1,3-substituted olefins and vinyl ethers under mild reaction conditions is possible provided a careful conformational search for TS structures is carried out and all the low energy conformers are taken into account. The internal energy can be used with satisfactory results to compute both the regio- and stereoselectivities in the hydroformylation of 1,1-dimethylethene and 1,3-substituted substrates, in the latter case due to the separation of the catalytic and substituent moieties.

Conversely, in the hydroformylation of 1,1-diphenylethene and 1,2-substituted substrates the regioselectivity on aliphatic olefins determined from the internal energy is in good agreement with the experiment for the lowest terms (Me and Et), while for iPr and tBu the computed ratios are both very close to 50:50 although favoring the experimentally determined most abundant species. The values become decidedly better using the free energy-based ratios, due to the entropic contribution of bulky groups.

When experimental and theoretical selectivities are not consistent, however, the products might undergo further reactions such as β-hydride elimination, in a few cases already elucidated via deuterioformylation experiments.

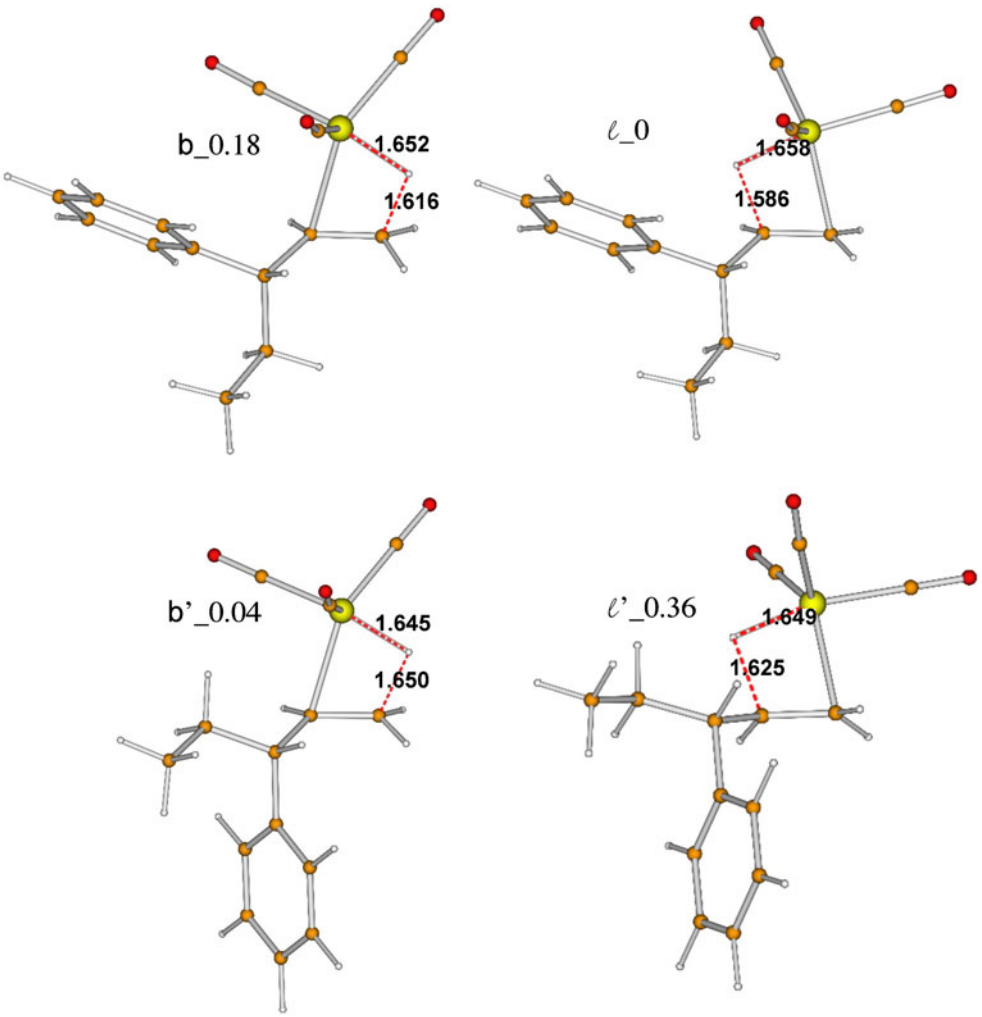

Fig. 5 B3P86/6-31G*/LanL2DZ most favorable branched and linear Rh-alkyl TS complexes for the (1-ethyl-ally)-benzene substrate (i.e., R=Φ). The TS structure type and relative stability (based on the internal energy, in kcal mol^{-1}) are also shown in the format type_Δ*E*

References

1. Anh NT, Eisenstein O (1977) Nouv J Chim 1:61–70
2. Houk KN (2000) Theor Chem Acc 103:330–331
3. Koga N, Jin SQ, Morokuma K (1988) J Am Chem Soc 110:3417–3425
4. Matsubara T, Koga N, Ding Y, Musaev DG, Morokuma K (1997) Organometallics 16:1065–1078
5. Gleich D, Schmid R, Herrmann WA (1998) Organometallics 17:4828–48347
6. Rocha WR, De Almeida WB (1998) Organometallics 17:1961–1967
7. Torrent M, Solà M, Frenking G (2000) Chem Rev 100:439–493
8. Rocha WR, De Almeida WB (2000) Int J Quantum Chem 78:42–51
9. Rocha WR, De Almeida WB (2000) J Comput Chem 21:668–674
10. Carbó JJ, Maseras F, Bo C, van Leeuwen PWNM (2001) J Am Chem Soc 123:7630–7637
11. Decker SA, Cundari TR (2001) Organometallics 20:2827–2841
12. Alagona G, Ghio C, Lazzaroni R, Settambolo R (2001) Organometallics 20:5394–5404
13. Decker SA, Cundari TR (2002) New J Chem 26:129–135
14. Landis CR, Uddin J (2002) J Chem Soc, Dalton Trans:729-742
15. Alagona G, Ghio C, Lazzaroni R, Settambolo R (2004) Inorg Chim Acta 357:2980–2988
16. Rocha WR (2004) J Mol Struct THEOCHEM 677:133–143
17. Gleich D, Hutter J (2004) Chem Eur J 10:2435–2444
18. Luo M, Tang D, Li M (2005) Int J Quantum Chem 105:108–123
19. Alagona G, Ghio C (2005) J Organomet Chem 690:2339–2350
20. Settambolo R, Rocchiccioli S, Lazzaroni R, Alagona G (2006) Lett Org Chem 3:10–12
21. Sparta M, Børve KJ, Jensen VR (2007) J Am Chem Soc 129:8487–8499
22. Alagona G, Ghio C, Rocchiccioli S (2007) J Mol Model 13:823–837
23. Ghio C, Lazzaroni R, Alagona G (2009) Eur J Inorg Chem:98-103
24. Shaharun MS, Dutta BK, Mukhtar H (2009) AIChE J 55:3221–3233
25. Tang D, Zhang Y, Hu C (2009) Chin J Chem 27:81–87
26. Lazzaroni R, Settambolo R, Alagona G, Ghio C (2010) Coord Chem Rev 254:696–706
27. Da Silva JCS, Dias RP, De Almeida WB, Rocha WR (2010) J Comput Chem 31:1986–2000
28. McQuarrie DA (2000) Statistical mechanics. University Science Book, Sausalito, CA
29. Frisch MJ, Trucks GW, Schlegel HB, Scuseria GE, Robb MA, Cheeseman JR, Montgomery JA, Vreven T, Kudin KN, Burant JC, Millam JM, Iyengar SS, Tomasi J, Barone V, Mennucci B, Cossi M, Scalmani G, Rega N, Petersson GA, Nakatsuji H, Hada M, Ehara M, Toyota K, Fukuda R, Hasegawa J, Ishida M, Nakajima T, Honda Y, Kitao O, Nakai H, Klene M, Li X, Knox JE, Hratchian HP, Cross JB, Bakken V, Adamo C, Jaramillo J, Gomperts R, Stratmann RE, Yazyev O, Austin AJ, Cammi R, Pomelli C, Ochterski JW, Ayala PY, Morokuma K, Voth GA, Salvador P, Dannenberg JJ, Zakrzewski VG, Dapprich S, Daniels AD, Strain MC, Farkas O, Malick DK, Rabuck AD, Raghavachari K, Foresman JB, Ortiz JV, Cui Q, Baboul AG, Clifford S, Cioslowski J, Stefanov BB, Liu G, Liashenko A, Piskorz P, Komaromi I, Martin RL, Fox DJ, Keith T, Al-Laham MA, Peng CY, Nanayakkara A, Challacombe M, Gill PMW, Johnson B, Chen W, Wong MW, Gonzalez C, Pople JA (2004) Gaussian 03, Revision C.02. Gaussian Inc, Wallingford, CT
30. Becke AD (1993) J Chem Phys 98:5648–5652
31. Perdew JP (1986) Phys Rev B 33:8822–8824
32. Hehre WJ, Radom L, PvR S, Pople JA (1986) Ab initio molecular orbital theory. Wiley, New York
33. Hay PJ, Wadt WR (1985) J Chem Phys 82:270–283
34. Lee C, Yang W, Parr RG (1988) Phys Rev B 37:785–789
35. Lazzaroni R, Settambolo R, Alagona G, Ghio C (manuscript in preparation)
36. Miller WH (1979) J Am Chem Soc 101:6810–6814
37. Rocchiccioli S (2006) Substrate-induced Diastereoselectivity in Rhodium-Catalyzed Hydroformylation. PhD Thesis, University of Pisa
38. van Leeuwen PWNM, Casey CP, Whiteker GT (2000) in Rhodium Catalyzed Hydroformylation; van Leeuwen PWNM, Claver C (eds) Kluwer CMC, Dordrecht, The Netherlands, p 96
39. Alagona G, Ghio C (manuscript in preparation)